

Author Query Form

Journal: Stat

Article: sta4301

Dear Author,

During the copyediting of your manuscript the following queries arose.

Please refer to the query reference call out numbers in the page proofs and respond to each by marking the necessary comments using the PDF annotation tools.

Please remember illegible or unclear comments and corrections may delay publication.

Many thanks for your assistance.

Query No.	Query	Remarks
Q1	AUTHOR: Please confirm that given names (Blue) and surnames/family names (Vermilion) have been identified correctly.	
Q2	AUTHOR: Please verify that the linked ORCID identifiers are correct for each author.	
Q3	AUTHOR: Please supply post code for this affiliation.	
Q4	AUTHOR: Please provide city location for references Abramowitz and Stegun (1972), Alegria et al. (2018), Hannan (2009), Prudnikov et al. (1986), Stein (2012), & Yaglom (2004).	
Q5	AUTHOR: Please provide volume for reference Kleiber (2017).	

Please confirm that the funding sponsor list below was correctly extracted from your article: that it includes all funders and that the text has been matched to the correct FundRef Registry organization names. If a name was not found in the FundRef registry, it may not be the canonical name form, it may be a program name rather than an organization name, or it may be an organization not yet included in FundRef Registry. If you know of another name form or a parent organization name for a “not found” item on this list below, please share that information.

FundRef name	FundRef Organization Name
Fondo Nacional de Desarrollo Científico y Tecnológico	not found

ORIGINAL ARTICLE

Cross-dimple in the cross-covariance functions of bivariate isotropic random fields on spheres

Alfredo Alegría^{ID}

Departamento de Matemática, Universidad Técnica Federico Santa María, Valparaíso, Chile

Correspondence

Alfredo Alegría, Universidad Técnica Federico Santa María, Avenida España 1680, Valparaíso, Chile.

Email: alfredo.alegría@usm.cl

Funding information

Fondo Nacional de Desarrollo Científico y Tecnológico, Grant/Award Number: 11190686

Multivariate random fields allow to simultaneously model multiple spatially indexed variables, playing a fundamental role in geophysical, environmental and climate disciplines. This paper introduces the concept of cross-dimple for bivariate isotropic random fields on spheres and proposes an approach to build parametric models that possess this attribute. Our findings are based on the spectral representation of the matrix-valued covariance function. We show that our construction is compatible with both the negative binomial and circular-Matérn bivariate families of covariance functions. We illustrate through simulation experiments that the models proposed in this work allow to achieve improvements in terms of predictive performance when a dimple-like intrinsic structure is present.

KEYWORDS

circular-matérn, covariance function, Gegenbauer polynomials, negative binomial, positive semidefinite, Schoenberg sequence

1 | INTRODUCTION

Multivariate random field models provide a mathematical architecture to assess the spatial uncertainty of multiple natural variables (Wackernagel, 2003), playing an important role in a wealth of applications, including the assessment of natural resources, environmental monitoring and precipitation forecast, amongst many others. This paper focuses on bivariate random fields on the d -dimensional unit sphere, denoted by $\mathbb{S}^d = \{\mathbf{s} \in \mathbb{R}^{d+1} : \mathbf{s}^T \mathbf{s} = 1\}$, for $d \in \mathbb{N}$, where T is the transpose operator. In particular, \mathbb{S}^2 can be used to approximate the globe, being of interest in Earth system sciences (Castruccio & Genton, 2014; Jeong, Jun, & Genton, 2017; Marinucci & Peccati, 2011; Porcu, Alegría, & Furrer, 2018).

Let $\{\mathbf{Z}(\mathbf{s}) = [Z_1(\mathbf{s}), Z_2(\mathbf{s})]^T : \mathbf{s} \in \mathbb{S}^d\}$ be a second-order, zero-mean, bivariate random field. We assume throughout that $\mathbf{Z}(\mathbf{s})$ is isotropic (Marinucci & Peccati, 2011); that is, there exists a matrix-valued function $\mathbf{K} : [0, \pi] \rightarrow \mathbb{R}^{2 \times 2}$, with (i, j) th entry given by $k_{ij} : [0, \pi] \rightarrow \mathbb{R}$, for $i, j = 1, 2$, such that

$$\text{cov}\{Z_i(\mathbf{s}), Z_j(\mathbf{s}')\} = k_{ij}(\vartheta),$$

where $\vartheta := \vartheta(\mathbf{s}, \mathbf{s}') = \arccos(\mathbf{s}^T \mathbf{s}') \in [0, \pi]$ is the geodesic distance between locations \mathbf{s} and \mathbf{s}' in \mathbb{S}^d . The diagonal and off-diagonal elements of \mathbf{K} are called marginal covariance and cross-covariance functions, respectively. The assumption of isotropy implies that the matrix-valued covariance function is symmetric: $k_{12}(\vartheta) = k_{21}(\vartheta)$, for all $\vartheta \in [0, \pi]$ (see, e.g., Alegría, Porcu, & Furrer, 2018). Positive semidefiniteness is a necessary and sufficient condition for \mathbf{K} to be an admissible covariance function (Genton & Kleiber, 2015). Valid parametric classes of covariance functions on spheres have been proposed by Gneiting (2013), Guinness and Fuentes (2016), Porcu, Bevilacqua, and Genton (2016), Alegría, Cuevas, Diggle, and Porcu (2018) and Emery and Porcu (2019).

In this work, we pay attention to cross-covariance functions with a cross-dimple, which is described as follows (a precise definition is given in Section 3). A cross-dimple is present if $Z_1(\mathbf{s}_{\text{here}})$ is more correlated with $Z_2(\mathbf{s}_{\text{there}})$ than with $Z_2(\mathbf{s}_{\text{here}})$. Although the occurrence of a dimple-like behaviour was originally studied for the temporal margins of space-time covariance functions (Alegría & Porcu, 2017; Cuevas, Porcu, & Bevilacqua, 2017; Kent, Mohammadzadeh, & Mosammam, 2011; Mosammam, 2015), we have noticed that the cross-covariance functions of (purely spatial) multivariate random fields can also possess this property. For anisotropic random fields, this behaviour can be attributed to a spatial delay between the components (Alegría et al. 2018; Li & Zhang, 2011). However, we are not aware of a similar notion for isotropic random fields.

Following several attempts to make multivariate spatial data modelling more flexible (Gneiting, Kleiber, & Schlather, 2010; Kleiber, 2017; Porcu, Bevilacqua, & Hering, 2018; Schlather, Malinowski, Menck, Oesting, & Strokorb, 2015), this paper proposes a strategy, based on the spectral

representation of the covariance function, for the construction of parametric isotropic models with the cross-dimple attribute. Our findings are accompanied by examples as well as simulation experiments that illustrate the improvements in predictive performance by using a covariance with cross-dimple.

The remainder of this paper is organized as follows. Background material about the spectral characterization of matrix-valued covariance functions on spheres is provided in Section 2. A definition of the cross-dimple, a spectral approach to model this property and some examples are presented in Section 3. Numerical experiments are illustrated in Section 4. Section 5 concludes the paper with a discussion.

2 | SPECTRAL REPRESENTATION OF COVARIANCE FUNCTIONS ON SPHERES

Let us briefly review preliminary material about the spectral representation of covariance functions on spheres. Any continuous covariance function $\mathbf{K} : [0, \pi] \rightarrow \mathbb{R}^{2 \times 2}$, associated with an isotropic, bivariate random field on \mathbb{S}^d , is characterized by the expansion (Hannan, 2009; Yaglom, 2004)

$$\mathbf{K}(\vartheta) = \begin{cases} \sum_{n=0}^{\infty} \mathbf{B}_{n,1} \cos(n\vartheta), & d = 1, \\ \sum_{n=0}^{\infty} \mathbf{B}_{n,d} c_{n,d}(\cos \vartheta), & d \geq 2, \end{cases} \quad (1)$$

where $\vartheta \in [0, \pi]$, and $\{\mathbf{B}_{n,d} : n \in \mathbb{N}_0\}$ is a sequence (referred to as a *Schoenberg sequence*) of positive semidefinite and (component-wise) summable 2×2 matrices. Here,

$$c_{n,d}(\cos \vartheta) = \frac{C_n^{(d-1)/2}(\cos \vartheta)}{C_n^{(d-1)/2}(1)},$$

with C_n^μ standing for the μ -Gegenbauer polynomial of degree n (Abramowitz & Stegun, 1972), which is defined in terms of its generating function,

$$\frac{1}{(1 - 2rt + t^2)^\mu} = \sum_{n=0}^{\infty} C_n^\mu(r) t^n,$$

where $-1 \leq r \leq 1$. When $d = 2$, the spectral expansion is expressed in terms of Legendre polynomials, $c_{n,2}(\cos \vartheta) = P_n(\cos \vartheta)$ (Abramowitz & Stegun, 1972).

The Schoenberg sequence fully characterizes the second-order spatial dependency of the random field. For univariate random fields, there is an analogous representation, for which Schoenberg matrices reduce to non-negative and summable scalars (Schoenberg, 1942).

Characterization (1) is parenthetical to the spectral representation of covariance functions on Euclidean spaces (Cramér, 1940).

3 | CROSS-DIMPLE THROUGH WEIGHTED SCHOENBERG SEQUENCES

We start by introducing a formal definition of the cross-dimple property for bivariate random fields on spheres.

Definition 1. Let $\mathbf{Z}(\mathbf{s})$ be an isotropic, bivariate random field on \mathbb{S}^d , with matrix-valued covariance function $\mathbf{K} : [0, \pi] \rightarrow \mathbb{R}^{2 \times 2}$. Then, we distinguish between two different cases.

- (1) We say that $k_{12}(\vartheta)$ has a positive cross-dimple if $k_{12}(0) \geq 0$ and if there exists $\vartheta_0 \in (0, \pi)$ such that $k_{12}(\vartheta)$ is increasing for $\vartheta \in (0, \vartheta_0)$.
- (2) We say that $k_{12}(\vartheta)$ has a negative cross-dimple if $k_{12}(0) \leq 0$ and if there exists $\vartheta_0 \in (0, \pi)$ such that $k_{12}(\vartheta)$ is decreasing for $\vartheta \in (0, \vartheta_0)$.

Observe that if $k_{12}(\vartheta)$ has a positive cross-dimple, then $-k_{12}(\vartheta)$ has a negative one. Hence, without loss of generality, we assume throughout that $k_{12}(0) \geq 0$.

We now present a general framework to construct covariance functions with a (positive) cross-dimple. First, consider a (dimple-less) covariance structure of the form

$$\mathbf{K}(\vartheta) = \begin{bmatrix} k_{11}(\vartheta) & k_{12}(\vartheta) \\ k_{12}(\vartheta) & k_{22}(\vartheta) \end{bmatrix} = \begin{bmatrix} \sigma_1^2 k(\vartheta; \xi_{11}) & \rho \sigma_1 \sigma_2 k(\vartheta; \xi_{12}) \\ \rho \sigma_1 \sigma_2 k(\vartheta; \xi_{12}) & \sigma_2^2 k(\vartheta; \xi_{22}) \end{bmatrix}, \quad (2)$$

where $\vartheta \in [0, \pi]$, $\rho \in (0, 1)$ is the colocated correlation coefficient between the components of the random field, $\sigma_i > 0$ is the standard deviation of the i th component and $\vartheta \mapsto k(\vartheta; \xi)$ is a valid univariate correlation function on the sphere. The vector of parameters is given by $[\sigma_1^2, \sigma_2^2, \rho, \xi_{11}, \xi_{12}, \xi_{22}]^T$. Two constructions of Type (2) (with appropriate restrictions on the parameters) will be analysed in Sections 3.1 and 3.2. The respective Schoenberg matrices, for $n \in \mathbb{N}_0$, can be written as

$$\mathbf{B}_{n,d} = \begin{bmatrix} \sigma_1^2 b_{n,d}(\xi_{11}) & \rho \sigma_1 \sigma_2 b_{n,d}(\xi_{12}) \\ \rho \sigma_1 \sigma_2 b_{n,d}(\xi_{12}) & \sigma_2^2 b_{n,d}(\xi_{22}) \end{bmatrix}, \quad (3)$$

for some sequence of non-negative numbers, $\{b_{n,d}(\xi) : n \in \mathbb{N}_0\}$, such that $\sum_{n=0}^{\infty} b_{n,d}(\xi) = 1$, for every ξ in the admissible parametric space. Recall that $\mathbf{B}_{n,d}$ is positive semidefinite for every $n \in \mathbb{N}_0$. Then, a modified cross-covariance function is obtained through a transformation of the Schoenberg sequence (3). Indeed, define $\tilde{\mathbf{K}}(\vartheta) : [0, \pi] \rightarrow \mathbb{R}^{2 \times 2}$ to be a matrix-valued covariance function characterized by the weighted Schoenberg matrices

$$\tilde{\mathbf{B}}_{n,d} = \begin{bmatrix} 1 & \lambda_n(\tau) \\ \lambda_n(\tau) & 1 \end{bmatrix} \circ \mathbf{B}_{n,d}, \quad (4)$$

where $n \in \mathbb{N}_0$, \circ denotes Hadamard (or Schur) product, and

$$\lambda_n(\tau) = 1\{n \leq \tau\} - 1\{n > \tau\}, \quad (5)$$

for $\tau \in \mathbb{N}_0$, with $1\{\cdot\}$ being the indicator function. The choice of τ , which is handled as an additional parameter, only impacts the cross-covariance structure of the random field (the marginal features are preserved). Of course, as $\tau \rightarrow \infty$, we recover the original covariance function.

Remark 1. The following comments guarantee that $\{\tilde{\mathbf{B}}_{n,d} : n \in \mathbb{N}_0\}$ is certainly a well-defined Schoenberg sequence.

a. Because $|\lambda_n(\tau)| = 1$, for all n and τ in \mathbb{N}_0 , one has

$$\left| \sum_{n=0}^{\infty} \lambda_n(\tau) b_{n,d}(\xi_{12}) \right| \leq \sum_{n=0}^{\infty} b_{n,d}(\xi_{12}) = 1.$$

In consequence, the matrices defined in (4) are component-wise summable.

b. The equality $\det(\tilde{\mathbf{B}}_{n,d}) = \det(\mathbf{B}_{n,d})$ implies that $\tilde{\mathbf{B}}_{n,d}$ is positive semidefinite.

Is there any choice of τ that leads to a cross-dimple? The following theorem provides an answer to this question.

Theorem 1. Consider a (dimple-less) cross-covariance function $k_{12}(\vartheta)$ as in (2), with the respective Schoenberg sequence $\{\rho\sigma_1\sigma_2 b_{n,d}(\xi_{12}) : n \in \mathbb{N}_0\}$. Suppose that

$$\eta := \sum_{n=0}^{\infty} \gamma_{n,d} b_{n,d}(\xi_{12}) < \infty, \quad (6)$$

where $\gamma_{n,d} = n(n+d-1)/d$. Then, the modified cross-covariance function $\tilde{k}_{12}(\vartheta)$, obtained from the weighted Schoenberg sequence $\{\lambda_n(\tau)\rho\sigma_1\sigma_2 b_{n,d}(\xi_{12}) : n \in \mathbb{N}_0\}$, has a (positive) cross-dimple if and only if there exists $\tau \in \mathbb{N}_0$ such that the following conditions hold.

$$(C1) \quad \sum_{n=0}^{\tau} b_{n,d}(\xi_{12}) \geq 1/2.$$

$$(C2) \quad \sum_{n=0}^{\tau} \gamma_{n,d} b_{n,d}(\xi_{12}) < \eta/2.$$

A proof of this theorem is given in Appendix B1. In summary, Theorem 1 establishes that the finite sum of the $(\tau+1)$ first terms of the sequence $\{b_{n,d}(\xi_{12}) : n \in \mathbb{N}_0\}$ must be greater than or equal to $1/2$. At the same time, when we consider the sequence $\{\gamma_{n,d} b_{n,d}(\xi_{12}) : n \in \mathbb{N}_0\}$, the sum of the $(\tau+1)$ first terms must be less than half the full sum. For example, when τ is arbitrarily large, Condition (C1) is fulfilled, but Condition (C2) is violated. The values of τ that satisfy both conditions will depend on the specific covariance function being studied. In the next subsections, we illustrate the use of this theorem on two parametric models.

3.1 | Example 1: Bivariate negative binomial covariance

The bivariate negative binomial covariance model on \mathbb{S}^2 has the form (Equation 2), with

$$k(\vartheta; \delta_{ij}) = \frac{1 - \delta_{ij}}{\sqrt{1 + \delta_{ij}^2 - 2\delta_{ij} \cos \vartheta}},$$

for $\vartheta \in [0, \pi]$ and $i, j = 1, 2$. The corresponding Schoenberg matrices, given in (3), are obtained from the sequence

$$b_{n,2}(\delta_{ij}) = (1 - \delta_{ij}) \delta_{ij}^n,$$

for $n \in \mathbb{N}_0$. This model is valid when $\delta_{11} < 1$, $\delta_{22} < 1$, $0 < \delta_{12} \leq \min(\delta_{11}, \delta_{22})$, and $|\rho| \leq \sqrt{(1 - \delta_{11})(1 - \delta_{22})}(1 - \delta_{12})^{-1}$ (Emery & Porcu, 2019). In order to study the occurrence of the cross-dimple for the negative binomial family, we look at Conditions (C1) and (C2) in Theorem 1, using standard results for geometric sequences.

• Notice that (C1) reduces to

$$\sum_{n=0}^{\tau} b_{n,2}(\delta_{12}) = (1 - \delta_{12}) \sum_{n=0}^{\tau} \delta_{12}^n = 1 - \delta_{12}^{\tau+1} \geq 1/2.$$

The last inequality yields the restriction $\tau \geq -1 - \log(2)/\log(\delta_{12})$.

• On the other hand, one has (see Prudnikov, Brychkov, & Marichev, 1986, chapter 4)

$$\sum_{n=0}^{\tau} \frac{n(n+1)}{2} b_{n,2}(\delta_{12}) = \frac{\delta_{12}}{2(1-\delta_{12})^2} [2\tau(\tau+2)\delta_{12}^{\tau+1} - \tau(\tau+1)\delta_{12}^{\tau+2} - (\tau+1)(\tau+2)\delta_{12}^{\tau} + 2],$$

and

$$\eta = \sum_{n=0}^{\infty} \frac{n(n+1)}{2} b_{n,2}(\delta_{12}) = \frac{\delta_{12}}{(1-\delta_{12})^2} < \infty.$$

Hence, (C2) reduces to

$$2\tau(\tau+2)\delta_{12} - \tau(\tau+1)\delta_{12}^2 - (\tau+2)(\tau+1) + \delta_{12}^{-\tau} < 0,$$

or equivalently,

$$\tau^2(\delta_{12} - 1)^2 + \tau(\delta_{12} - 3)(\delta_{12} - 1) + 2 > \delta_{12}^{-\tau}.$$

In Figure 1 (left), we show the combinations of δ_{12} and τ where Conditions (C1) and (C2) are satisfied. For example, when $\delta_{12} = 0.65$, a dimple occurs for $\tau \in \{1, \dots, 5\}$. Instead, when $\delta_{12} = 0.8$, it occurs for $\tau \in \{3, \dots, 11\}$. It is not possible to achieve a cross-dimple when $\delta_{12} \rightarrow 1$. Of course, this limit case is of little interest. Figure 1 (right) displays the negative binomial covariance function, with $\delta_{11} = 0.8$, $\delta_{22} = 0.7$, $\delta_{12} = 0.65$, $\sigma_1 = \sigma_2 = 1$ and $\rho = 0.65$, and the modified cross-covariance functions for different values of τ . The dimple-like behaviour is clearly visible. As τ increases, the cross-dimple gradually disappears.

F1

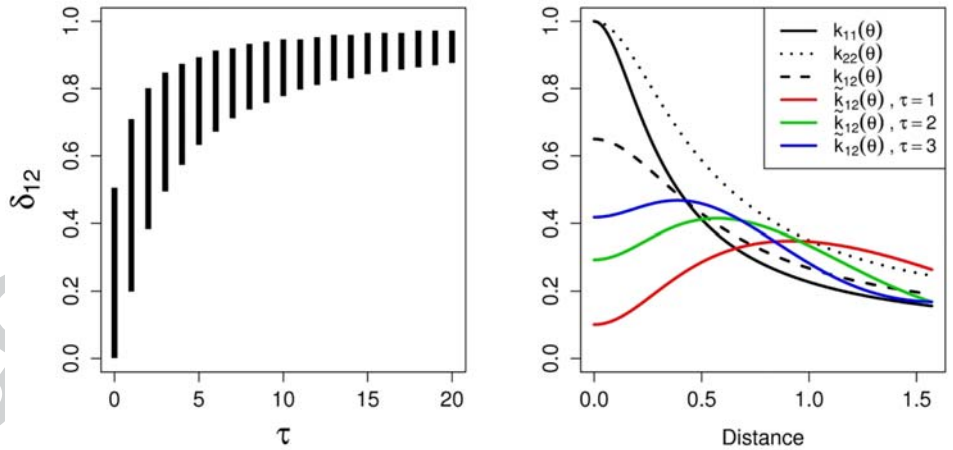


FIGURE 1 (Left) The black zone shows the combinations of δ_{12} and τ , in the modified negative binomial family, which leads to a cross-dimple. (Right) Negative binomial covariance function, with $\delta_{11} = 0.8$, $\delta_{22} = 0.7$, $\delta_{12} = 0.65$, $\sigma_1 = \sigma_2 = 1$ and $\rho = 0.65$, and the modified cross-covariance functions for different values of τ

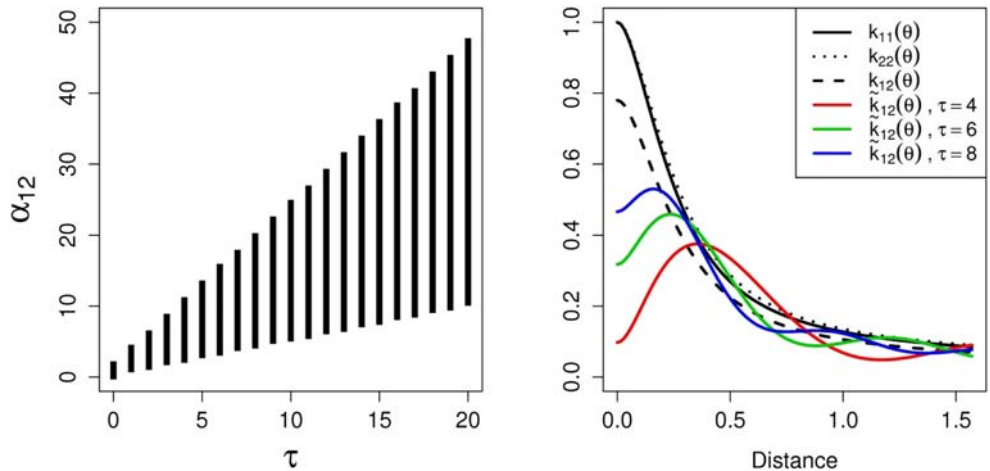


FIGURE 2 (Left) The black zone shows the combinations of α_{12} and τ that leads to a cross-dimple in the modified circular-Matérn family. (Right) Circular-Matérn covariance function, with $\alpha_{11} = 10$, $\alpha_{22} = \alpha_{12} = 9.4$, $\sigma_1 = \sigma_2 = 1$ and $\rho = 0.78$, and the modified cross-covariance functions for different values of τ

3.2 | Example 2: Bivariate circular-matérn covariance

The bivariate circular-Matérn covariance function on \mathbb{S}^2 (Emery & Porcu, 2019; Guinness & Fuentes, 2016) is a model of Form (2). The respective Schoenberg matrices, as in (3), are obtained from the sequence

$$b_{n,2}(\alpha_{ij}, \nu) = \frac{1}{S(\alpha_{ij}, \nu)(n^2 + \alpha_{ij}^2)^{\nu+1/2}}, \quad (7)$$

for $n \in \mathbb{N}_0$ and $i, j = 1, 2$, where

$$S(\alpha_{ij}, \nu) = \sum_{\ell=0}^{\infty} \frac{1}{(\ell^2 + \alpha_{ij}^2)^{\nu+1/2}}.$$

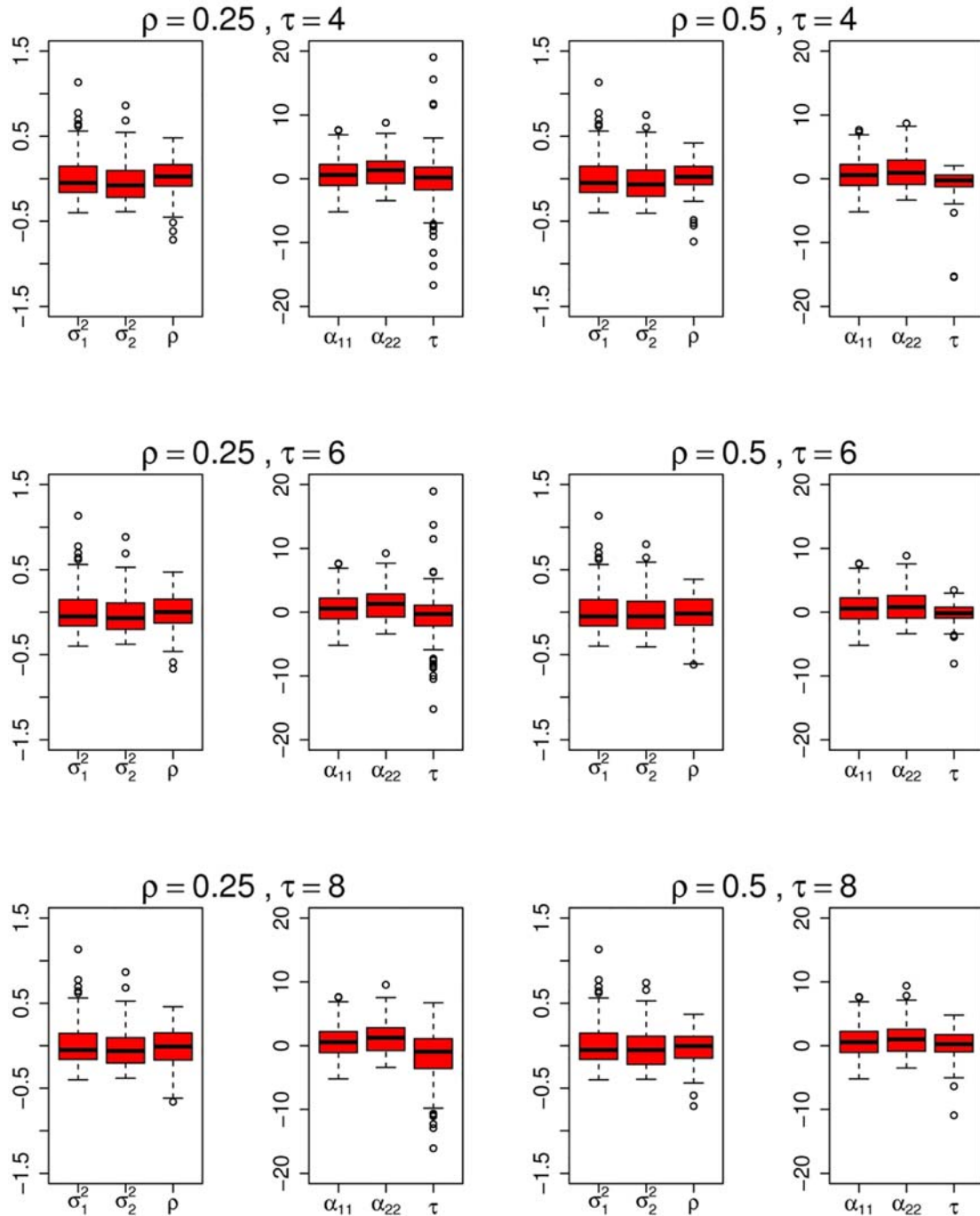


FIGURE 3 Bias of the pairwise likelihood estimates for the CM-D model, with $\sigma_1^2 = \sigma_2^2 = 1$, $\alpha_{11} = 10$, $\alpha_{22} = 9.4$ and $(\rho, \tau) \in \{0.25, 0.5\} \times \{4, 6, 8\}$. Here, $\alpha_{12} = \min(\alpha_{11}, \alpha_{22})$ and $\nu = 3/2$ are fixed. Because parameters have different scales of variation, the estimates of $(\sigma_1^2, \sigma_2^2, \rho)$ and $(\alpha_{11}, \alpha_{22}, \tau)$ are given separately

TABLE 1 Cross-validation scores for the circular-Matérn (CM) and circular-Matérn with cross-dimple (CM-D) models, when the inherent structure is of CM-D type, with $\sigma_1^2 = \sigma_2^2 = 1$, $\alpha_{11} = 10$, $\alpha_{22} = 9.4$ and $(\rho, \tau) \in \{0.25, 0.5\} \times \{4, 6, 8\}$

		MSPE		LSCORE		CRPS	
		CM	CM-D	CM	CM-D	CM	CM-D
$\tau = 4$	$\rho = 0.25$	0.183	0.163	0.507	0.448	0.848	0.820
	$\rho = 0.5$	0.209	0.136	0.643	0.407	0.861	0.755
$\tau = 6$	$\rho = 0.25$	0.189	0.164	0.529	0.451	0.850	0.823
	$\rho = 0.5$	0.232	0.138	0.732	0.378	0.866	0.764
$\tau = 8$	$\rho = 0.25$	0.191	0.167	0.537	0.455	0.852	0.826
	$\rho = 0.5$	0.241	0.139	0.781	0.375	0.869	0.767

Note: Here, $\alpha_{12} = \min(\alpha_{11}, \alpha_{22})$ and $\nu = 3/2$ are fixed.

Abbreviations: CRPS, continuous ranked probability score; LSCORE, log-score; MSPE, mean-squared prediction error.

Unlike the negative binomial class, this covariance function does not have a closed form. Following Emery and Porcu (2019), the circular-Matérn covariance is valid when $0 < \alpha_{12} \leq \min(\alpha_{11}, \alpha_{22})$, $\nu > 0$, and

$$|\rho| \leq \frac{S(\alpha_{12}, \nu)^2}{S(\alpha_{11}, \nu)S(\alpha_{22}, \nu)} \left(\frac{\alpha_{12}^2}{\alpha_{11}\alpha_{22}} \right)^{2\nu+1}.$$

We now investigate the occurrence of the cross-dimple in the circular-Matérn family. Conditions (C1) and (C2) in Theorem 1 cannot be written in closed form, so they will be explored numerically. Assumption (6) in Theorem 1 holds for any $\nu > 1$. We fix $\nu = 3/2$. The combinations of α_{12} and τ , where (C1) and (C2) are fulfilled, are reported in Figure 2 (left). For example, when $\alpha_{12} = 9$, a dimple occurs for $\tau \in \{4, \dots, 18\}$. The minimum and maximum values of τ increase with α_{12} . At first sight, this relationship seems to be linear; however, the increments are not constant. Figure 2 (right) illustrates the circular-Matérn covariance function, with $\alpha_{11} = 10$, $\alpha_{22} = \alpha_{12} = 9.4$, $\sigma_1 = \sigma_2 = 1$ and $\rho = 0.78$, and the modified cross-covariance functions for different values of τ . Again, as τ increases, the sharpness of the cross-dimple decreases. Also, an oscillating behaviour is present in the tails of the curves.

4 | SIMULATION STUDY

We conduct simulation studies related to bivariate Gaussian random fields on \mathbb{S}^2 . The circular-Matérn (CM) and circular-Matérn with cross-dimple (CM-D) models are considered. First, we assess the performance of likelihood-based inference for the CM-D model. In particular, we employ the pairwise likelihood method proposed by Bevilacqua, Alegria, Velandia, and Porcu (2016). In our experiments, we replace the discontinuous weight in (5) by a logistic function of the form $\lambda_n(\tau) = 1 - 2[1 + \exp(-5(n - \tau))]^{-1}$, which captures the desired dichotomic structure. Thus, τ is handled as a continuous parameter, while keeping the same values for the modified Schoenberg sequence. We simulate 100 independent realizations of a bivariate random field, on a spatial grid of longitudes and latitudes of size 30×15 , with a CM-D covariance function. We set $\sigma_1^2 = \sigma_2^2 = 1$, $\alpha_{11} = 10$, $\alpha_{22} = 9.4$ and $(\rho, \tau) \in \{0.25, 0.5\} \times \{4, 6, 8\}$, which leads to six different scenarios. Here, $\alpha_{12} = \min(\alpha_{11}, \alpha_{22})$ and $\nu = 3/2$ are fixed. In our implementation, the Schoenberg series are truncated after 200 terms. Figure 3 displays the centred boxplots of the estimates for each scenario. Overall, the boxplots show that direct maximization of the objective function provides quite reasonable estimations. For $\rho = 0.25$, the correlation between the components of the random field is weaker, causing a slight bias in the estimates of τ . Instead, for $\rho = 0.5$, this bias disappears. A two-step estimation approach as in Li and Zhang (2011) may also be adopted to avoid a maximization problem with a large number of parameters.

We turn to a cross-validation study to compare the predictive performance of the CM and CM-D models under a dimple-like inherent structure. For 100 independent realizations from the CM-D model, we quantify the accuracy of the cokriging predictor through the mean-squared prediction error (MSPE), the log-score (LSCORE) and the continuous ranked probability score (CRPS) (see Zhang & Wang, 2010). These indicators are evaluated using a drop-one prediction strategy. Table 1 reports the results for the scenarios described above. It is clear that the CM-D model provides better results than does the CM model. Notice that for $\rho = 0.5$, the improvements are more significant. This is not surprising because under this choice, the correlation between the components of the random field is stronger; thus, the accuracy of the prediction is more sensitive to an incorrect specification of the cross-dependency structure.

5 | DISCUSSION

We proposed a spectral methodology to build cross-covariance functions with a cross-dimple. The compatibility of our approach with two existing families of covariance functions has been verified. The estimation of our models has been illustrated through simulation experiments. Also, we showed that when a cross-dimple is present, ignoring this attribute will result in inferior predictions.

To understand the physical meaning of this property is an intriguing research challenge that deserves more attention. We expect to study the occurrence of the cross-dimple in real data applications. In the work of Hewson, McGowan, Phinn, Peckham, and Grell (2013), some visual hints about the presence of a cross-dimple can be identified in the empirical cross-variograms of rain events.

An extension of this work to the case of p -variate random fields, with $p > 2$, is straightforward, because any off-diagonal entry of the matrix-valued covariance function can be modified along the lines of Section 3. The search for connections between the cross-dimple and the coherence function discussed by Kleiber (2017) is a promising topic for future research. The cross-dimple is not only limited to the spherical context. Bivariate random fields on Euclidean spaces can also exhibit this property. To address this problem, the spectral characterization of covariance functions on Euclidean spaces is fundamental (Cramér, 1940). In this context, the Matérn class of covariance functions (Gneiting et al. 2010; Laga & Kleiber, 2017; Stein, 2012) is the most popular alternative, so that the inclusion of a cross-dimple in a cross-covariance function of Matérn type is an interesting problem that we expect to tackle in the future.

ACKNOWLEDGEMENTS

The author is grateful to two anonymous reviewers and an associate editor for their constructive comments.

FUNDING INFORMATION

This research was supported by Grant FONDECYT 11190686 from the Chilean government.

DATA AVAILABILITY STATEMENT

The simulated data that support the findings of this study are available from the corresponding author upon reasonable request.

ORCID

Alfredo Alegría  <https://orcid.org/0000-0001-9720-7697>

REFERENCES

- Abramowitz, M., & Stegun, I. A. (1972). *Handbook of mathematical functions with formulas, graphs, and Mathematical tables*: Dover Publications.
- Alegría, A., & Porcu, E. (2017). The dimple problem related to space-time modeling under the Lagrangian framework. *Journal of Multivariate Analysis*, 162, 110–121.
- Alegría, A., Porcu, E., & Furrer, R. (2018). Asymmetric matrix-valued covariances for multivariate random fields on spheres. *Journal of Statistical Computation and Simulation*, 88(10), 1850–1862.
- Alegría, A., Cuevas, F., Diggle, P., & Porcu, E. (2018). A family of covariance functions for random fields on spheres. (CSGB Research Reports): Department of Mathematics, Aarhus University.
- Bevilacqua, M., Alegría, A., Velandia, D., & Porcu, E. (2016). Composite likelihood inference for multivariate Gaussian random fields. *Journal of Agricultural, Biological, and Environmental Statistics*, 21(3), 448–469.
- Castruccio, S., & Genton, M. G. (2014). Beyond axial symmetry: An improved class of models for global data. *Stat*, 3(1), 48–55.
- Cramér, H. (1940). On the theory of stationary random processes. *Annals of Mathematics*, 41, 215–230.
- Cuevas, F., Porcu, E., & Bevilacqua, M. (2017). Contours and dimple for the Gneiting class of space-time correlation functions. *Biometrika*, 104(4), 995–1001.
- Emery, X., & Porcu, E. (2019). Simulating isotropic vector-valued Gaussian random fields on the sphere through finite harmonics approximations. *Stochastic Environmental Research and Risk Assessment*, 33(8–9), 1659–1667.
- Genton, M. G., & Kleiber, W. (2015). Cross-covariance functions for multivariate geostatistics. *Statistical Science*, 30(2), 147–163.
- Gneiting, T. (2013). Strictly and non-strictly positive definite functions on spheres. *Bernoulli*, 19(4), 1327–1349.
- Gneiting, T., Kleiber, W., & Schlather, M. (2010). Matérn cross-covariance functions for multivariate random fields. *Journal of the American Statistical Association*, 105(491), 1167–1177.
- Guinness, J., & Fuentes, M. (2016). Isotropic covariance functions on spheres: some properties and modeling considerations. *Journal of Multivariate Analysis*, 143, 143–152.
- Hannan, E. J. (2009). *Multiple time series*. Wiley series in probability and statistics: Wiley.
- Hewson, M., McGowan, H., Phinn, S., Peckham, S., & Grell, G. (2013). Exploring aerosol effects on rainfall for Brisbane, Australia. *Climate*, 1(3), 120–147.
- Jeong, J., Jun, M., & Genton, M. G. (2017). Spherical process models for global spatial statistics. *Statistical Science*, 32(4), 501–513.
- Kent, J. T., Mohammadzadeh, M., & Mosammam, A. M. (2011). The dimple in Gneiting's spatial-temporal covariance model. *Biometrika*, 98, 489–494.
- Kleiber, W. (2017). Coherence for multivariate random fields. *Statistica Sinica*, 1675–1697.
- Laga, I., & Kleiber, W. (2017). The modified Matérn process. *Stat*, 6(1), 241–247.
- Li, B., & Zhang, H. (2011). An approach to modeling asymmetric multivariate spatial covariance structures. *Journal of Multivariate Analysis*, 102(10), 1445–1453.
- Marinucci, D., & Peccati, G. (2011). *Random fields on the sphere: representation, limit theorems and cosmological applications*. Cambridge: Cambridge University Press.
- Mosammam, A. M. (2015). The reverse dimple in potentially negative-value space-time covariance models. *Stochastic Environmental Research and Risk Assessment*, 29(2), 599–607.
- Porcu, E., Alegría, A., & Furrer, R. (2018). Modeling temporally evolving and spatially globally dependent data. *International Statistical Review*, 86(2), 344–377.
- Porcu, E., Bevilacqua, M., & Genton, M. G. (2016). Spatio-temporal covariance and cross-covariance functions of the great circle distance on a sphere. *Journal of the American Statistical Association*, 111(514), 888–898.
- Porcu, E., Bevilacqua, M., & Hering, A. S. (2018). The Shkarofsky–Gneiting class of covariance models for bivariate Gaussian random fields. *Stat*, 7(1), e207.

Q4

Q5

- Prudnikov, A. P., Brychkov, Y. A., & Marichev, O. I. (1986). *Integrals and series [vol 1—Elem. functions]*: Gordon and Breach Science Publishers.
- Schlather, M., Malinowski, A., Menck, P. J., Oesting, M., & Strokorb, K. (2015). Analysis, simulation and prediction of multivariate random fields with package RandomFields. *Journal of Statistical Software*, 63(8), 1–25.
- Schoenberg, I. J. (1942). Positive definite functions on spheres. *Duke Mathematical Journal*, 9(1), 96–108.
- Stein, M. L. (2012). *Interpolation of spatial data: Some theory for kriging*: Springer Science & Business Media.
- Wackernagel, H. (2003). *Multivariate geostatistics: An introduction with applications* (3rd ed.). New York: Springer.
- Yaglom, A. M. (2004). *An introduction to the theory of stationary random functions*: Courier Corporation.
- Zhang, H., & Wang, Y. (2010). Kriging and cross-validation for massive spatial data. *Environmetrics*, 21(3/4), 290–304.

How to cite this article: Alegría A. Cross-dimple in the cross-covariance functions of bivariate isotropic random fields on spheres. *Stat.* 2020;9:e301. <https://doi.org/10.1002/sta4.301>

APPENDIX A: PROOF OF THEOREM 1

The proof consists of two parts.

- First, we verify that $\tilde{k}_{12}(0) \geq 0$. Notice that for $\rho \in (0, 1)$,

$$\tilde{k}_{12}(0) = \rho\sigma_1\sigma_2 \sum_{n=0}^{\infty} \lambda_n(\tau) b_{n,d}(\xi_{12}) = \rho\sigma_1\sigma_2 \left(\sum_{n=0}^{\tau} b_{n,d}(\xi_{12}) - \sum_{n=\tau+1}^{\infty} b_{n,d}(\xi_{12}) \right). \quad (\text{A1})$$

From (C1), one has

$$2 \sum_{n=0}^{\tau} b_{n,d}(\xi_{12}) \geq \sum_{n=0}^{\infty} b_{n,d}(\xi_{12}) = 1.$$

Subtracting $\sum_{n=0}^{\tau} b_{n,d}(\xi_{12})$ from both sides of the last inequality, we conclude that (A1) is non-negative.

- Second, we calculate the first-order derivative of $\tilde{k}_{12}(\vartheta)$ at a neighbourhood of zero. Assumption (6) is key to swap series with derivatives. We focus on the case where $d \geq 2$ (the one-dimensional case is similar). We take advantage of the following identities (Abramowitz & Stegun, 1972):

$$C_n^{\mu}(1) = \frac{\Gamma(n+2\mu)}{n!\Gamma(2\mu)} \quad \text{and} \quad \frac{d}{dx} C_n^{\mu}(x) = 2\mu C_{n-1}^{\mu+1}(x).$$

A direct calculation shows that

$$\begin{aligned} \frac{d}{d\vartheta} \tilde{k}_{12} &= -(\sin \vartheta) \rho\sigma_1\sigma_2 \sum_{n=0}^{\infty} \lambda_n(\tau) b_{n,d}(\xi_{12}) (d-1) \frac{C_{n-1}^{(d+1)/2}(\cos \vartheta)}{C_n^{(d-1)/2}(1)} \\ &= (\sin \vartheta) \rho\sigma_1\sigma_2 \left[- \sum_{n=0}^{\tau} b_{n,d}(\xi_{12}) (d-1) \frac{C_{n-1}^{(d+1)/2}(\cos \vartheta)}{C_n^{(d-1)/2}(1)} \right. \\ &\quad \left. + \sum_{n=\tau+1}^{\infty} b_{n,d}(\xi_{12}) (d-1) \frac{C_{n-1}^{(d+1)/2}(\vartheta)}{C_n^{(d-1)/2}(1)} \right]. \end{aligned} \quad (\text{A2})$$

Observe that

$$(d-1) \frac{C_{n-1}^{(d+1)/2}(1)}{C_n^{(d-1)/2}(1)} = \frac{n(n+d-1)}{d} = \gamma_{n,d}.$$

Thus, as ϑ goes to zero, the term in brackets in (A2) tends to

$$- \sum_{n=0}^{\tau} b_{n,d}(\xi_{12}) \gamma_{n,d} + \sum_{n=\tau+1}^{\infty} b_{n,d}(\xi_{12}) \gamma_{n,d}. \quad (\text{A3})$$

From Condition (C2), we conclude that (A3) is positive. In conclusion, $\tilde{k}_{12}(\vartheta)$ is locally increasing on an interval of the form $(0, \vartheta_0)$, for some $\vartheta_0 \in (0, \pi)$.